

2 Novel Application of Laboratory 3 Instrumentation Characterizes Mass Settling 4 Dynamics of Oil-Mineral Aggregates (OMAs) 5 and Oil-Mineral-Microbial Interactions

6 AUTHORS

7 **Leiping Ye**

8 University of Delaware

9 **Andrew J. Manning**

10 University of Delaware

11 HR Wallingford Ltd., Coasts and

12 Oceans Group, Wallingford, UK

13 University of Hull

14 University of Plymouth

15 **Tian-Jian Hsu**

16 University of Delaware

17 **Steve Morey**

18 Florida A&M University

19 Florida State University

20 **Eric P. Chassignet**

21 **Tracy A. Ippolito**

22 Florida State University

39 ABSTRACT

40 It is reasonable to assume that microbes played an important role in determining
41 the eventual fate of oil spilled during the 2010 *Deepwater Horizon* disaster, given
42 that microbial activities in the Gulf of Mexico are significant and diverse. However,
43 critical gaps exist in our knowledge of how microbes influence the biodegradation
44 and accumulation of petroleum in the water column and in marine sediments of the
45 deep ocean and the shelf. Ultimately, this limited understanding impedes the ability to
46 forecast the fate of future oil spills, specifically the capacity of numerical models to
47 simulate the transport and fate of petroleum under a variety of conditions and regimes.

48 By synthesizing recent model developments and results from field- and laboratory-
49 based microbial studies, the Consortium for Simulation of Oil-Microbial Interactions
50 in the Ocean (CSOMIO) investigates (a) how microbial biodegradation influences
51 accumulation of petroleum in the water column and in marine sediments and
52 (b) how biodegradation can be influenced by environmental conditions and impact
53 forecasts of potential future oil spills.

54 **Keywords:**

23 Laboratory Flocculation 24 Experiments

25 Critical to oil-mineral-microbial
26 interactions is a process whereby cohe-
27 sive sediment particles do not behave
28 as individual, dispersed particles but
29 instead tend to stick together. This
30 process is known as flocculation, and
31 the resultant floc sizes and settling
32 velocity are much greater than those
33 of the individual constituent parti-
34 cles, but their overall floc effective
35 density is less (e.g., Dyer & Manning,
36 1999; Manning & Dyer, 1999).
37 When oil droplets are contained by
38 flocs of cohesive sediment and/or

55 marine snows, oil sedimentation can
56 occur and provide an unexpected
57 pathway in the oil budget calculation
58 (Daly et al., 2016; Muschenheim &
59 Lee, 2002; Passow & Ziervogel,
60 2016). A novel high-resolution floc
61 video instrument originally designed
62 to determine the spectral characteris-
63 tics of flocculating cohesive sediments
64 has, for the first time, been applied to
65 study floc size distribution and set-
66 tling dynamics of oil-mineral aggre-
67 gates (OMAs). The results of this
68 study inform the development of
69 efficient and accurate algorithms for
70 simulating the formation and settling
71 of these flocs.

72 As part of the Consortium for
73 Simulation of Oil-Microbial Inter-
74 actions in the Ocean (CSOMIO), a
75 series of laboratory flocculation exper-
76 iments with seawater, crude oil, and
77 cohesive sediment mixtures (mineral
78 clay and artificial extracellular poly-
79 meric substances) have been conducted
80 at the Center for Applied Coastal Re-
81 search, University of Delaware, using
82 the LabSFLOC-2 (the second genera-
83 tion of the LabSFLOC [Laboratory
84 Spectral Flocculation Characteristics
85 instrument; Manning, 2015], devel-
86 oped by Manning, 2006). In these
87 experiments, the LabSFLOC-2 instru-
88 ment, a digital video microscope and

Q1

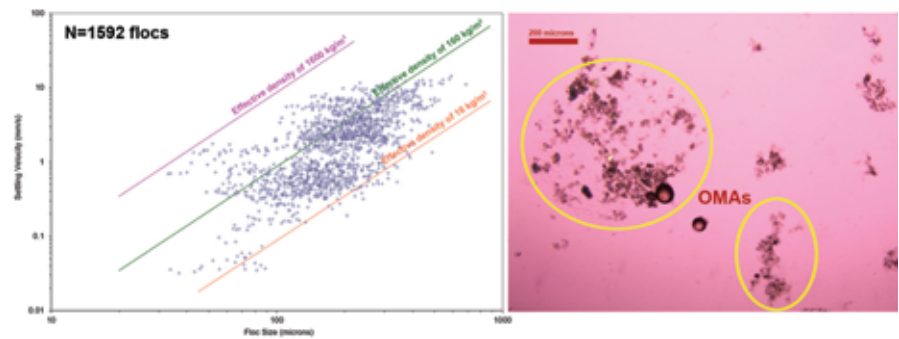
89 processing package, makes it possible to
 90 obtain high-quality floc population
 91 data (e.g., individual floc size, settling
 92 velocity, density, mass), as well as sup-
 93 plementary individual floc information
 94 including floc porosity, floc mass, frac-
 95 tal dimension, floc shape, and mass
 96 settling flux. Manning et al. (2010)
 97 and Manning et al. (2017) provide
 98 further details of the floc acquisition
 99 procedures and postprocessing compu-
 100 tations, respectively. LabSFLOC-2
 101 provides data for many important as-
 102 pects of flocculation. These floc data
 103 are necessary to comprehensively assess
 104 and characterize oil-mineral-microbial
 105 settling dynamics and to improve the
 106 parameterization (Manning & Dyer,
 107 2007; Soulsby et al., 2013) and calibra-
 108 tion (Baugh & Manning, 2007) of
 109 numerical models. Additionally, the
 110 digital microscope images help us better
 111 understand the visible floc structure of
 112 OMAs.

113 Laboratory Experiments 114 Utilizing the 115 LabSFLOC-2 Instrument

116 Mass settling dynamics of oil-
 117 mineral flocs are observed using the
 118 LabSFLOC-2 system (Figure 1),
 119 which measures an entire floc popula-
 120 tion for each sample being assessed.
 121 LabSFLOC-2 utilizes a low intrusive
 122 2.0-MP Grasshopper monochrome
 123 digital video camera to optically ob-
 124 serve individual flocs (e.g., Manning
 125 & Dyer, 2002) as they settle in a
 126 350 mm high \times 100 mm square
 127 Perspex settling column. The video
 128 camera, positioned nominally 75 mm
 129 above the base of the column, views
 130 all particles in the center of the column
 131 that pass within a 1-mm depth of field,
 132 45 mm from the Sill TZM 1560 high-
 133 magnification (nominal 5- μ m pixel
 134 resolution) telecentric (maximum

FIGURE 1

The LabSFLOC-2 setup on the desk beside the stir jar system for real-time samplings (photo provided by Prof. A. J. Manning).



135 pixel distortion of 0.6%), 0.66 (1:1.5)
 136 magnification, F4, macro lens.

137 A suspension containing oil-mineral-
 138 microbial flocs is initially introduced
 139 to the LabSFLOC-2 column, while a
 140 suspension is extracted from the
 141 jar fluid using a specially modified
 142 Serological TD-EX 20°C 50-ml
 143 maximum-capacity sterile pipette.
 144 This process has proved to be mini-
 145 mally intrusive for flocs, relying only
 146 upon settling due to gravity and thus
 147 avoiding the need for additional
 148 fluid or turbulence transfer. The
 149 LabSFLOC-2 instrumentation is
 150 located close and adjacent to the stir
 151 jar system, as this minimizes the time
 152 needed to transfer floc samples to the
 153 LabSFLOC-2 settling chamber and
 154 any potential disruption during the
 155 subsequent floc settling process.

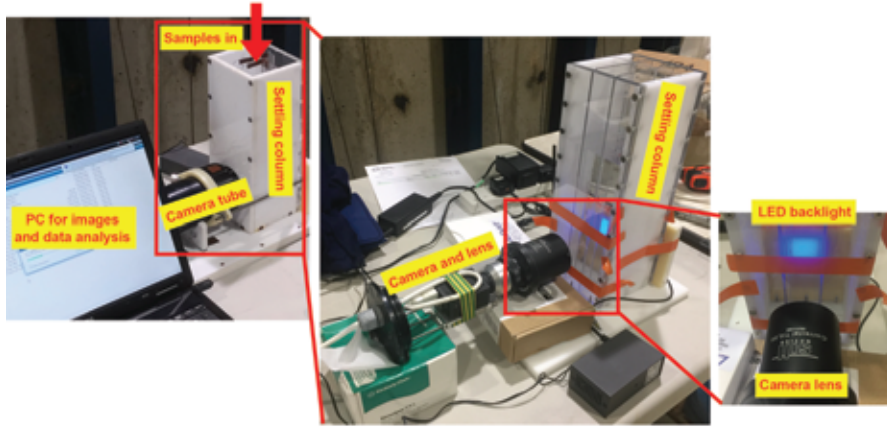
156 The camera views through an aper-
 157 ture in the settling column wall at a
 158 depth of 230 mm below the column
 159 water surface. It records all settling
 160 flocs/particles in the center of the
 161 column, which pass within a 1-mm
 162 focal depth of field, 45 mm (focal
 163 length) from the camera lens. The
 164 total image size is nominally 6 mm
 165 high and 8 mm wide. During sam-
 166 pling, a pipette is filled to produce a
 167 fluid head of 50 mm, which results in

168 a video image control sample volume
 169 nominally of 400 mm³ (1-mm image
 170 depth and 6-mm nominal video
 171 image width, with a nominal 50-mm
 172 high suspension extracted with a mod-
 173 ified pipette). This control volume
 174 permits the LabSFLOC-2 calculated
 175 total floc mass to be accurately mass-
 176 balanced with the nominal suspended
 177 particulate matter concentration uti-
 178 lized in the jar test under examination.
 179 The LabSFLOC-2 camera can view
 180 particles as small as 5 μ m and as large
 181 as 8 mm. Settling velocities ranging
 182 from 0.01 to 45 mm·s⁻¹ can be mea-
 183 sured by the LabSFLOC-2, and the
 184 system can operate within floc sus-
 185 pended particulate matter concentra-
 186 tions of a few milligrams per liter,
 187 with a practical upper operating limit
 188 of ~200 g·l⁻¹.

189 Settling flocs are viewed as silhou-
 190 ettes (to reduce image smearing) result-
 191 ing from a 43 \times 35 mm, homogeneous
 192 blue (470 nm), back-illumination
 193 LED panel located at the rear of the
 194 settling column. The digital floc im-
 195 ages are captured as non-Codec com-
 196 pressed AVI files at a frame rate of
 197 7.5 Hz (one frame is 0.04 s), at a reso-
 198 lution of 1,600 \times 1,200 pixels, with an
 199 individual pixel nominally represent-
 200 ing 5 μ m (confirmed by independent

FIGURE 2

Sample from an oil-bentonite case. The left plot shows the floc size and settling velocity scatters of each calculated floc. The three diagonal lines present contours of Stokes settling velocity calculated with a constant effective density (i.e., floc bulk density minus water density): pink = $1,600 \text{ kg}\cdot\text{m}^{-3}$ (equivalent to a quartz particle), green = $160 \text{ kg}\cdot\text{m}^{-3}$, and red = $16 \text{ kg}\cdot\text{m}^{-3}$. The right image is the generated OMAs as seen by the digital microscope camera (approximately $\times 40$).



calibration), connected and streamed to a laptop PC, and recorded on the internal hard drive.

The present system not only produces visible floc individual images (e.g., Figure 2, right) but also reveals all other essential quantitative floc properties. The uncompressed images are then analyzed with MATLAB software routines. During postprocessing, the HR Wallingford Ltd. DigiFloc software version 1.0 (Benson & Manning, 2013) and JavaScript can be used to semiautomatically process the digital recording image stack to obtain floc size and settling velocity spectra (e.g., Figure 2, left for oil-bentonite flocs). A modified version of Stokes' law (Stokes, 1851) permits an accurate estimate of individual floc effective density (Manning et al., 2013), which can then be utilized to calculate floc mass. In the oil-bentonite sample, resultant floc sizes (nominally mass-balanced to a suspended particulate matter concentration of $1,000\text{-mg}\cdot\text{l}^{-1}$ bentonite and 1 ml of Texas crude oil) ranged between

30 and $700 \mu\text{m}$, and settling velocities spanned $0.3\text{--}10 \text{ mm}\cdot\text{s}^{-1}$. The plot (Figure 2, left) shows a significant portion of the floc population clusters within the low-effective density ($16\text{--}160 \text{ kg}\cdot\text{m}^{-3}$) region.

Summary

In the first attempt to apply the LabSFLOC-2 system in an oil-mineral flocculation study, we have combined state-of-the-art technologies/instruments in order to expand our knowledge of oil-sediment-microbial interactions and the vertical transport of oil. The preliminary laboratory experiments demonstrate that these systems can be used to produce and characterize mass settling dynamics of OMAs. Future experiments will use different oil, sediment, and microbial characteristics and turbulence levels. Statistical data on settling dynamics provided by LabSFLOC-2 will allow for a systematic analysis of the role that each factor plays in determining the resultant settling dynamics. Mov-

ing forward, these technologies have the potential for applications to a carefully designed test matrix in order to calibrate a given modeling framework for oil-sediment-microbial interactions.

Acknowledgments

This research was made possible by a grant from the Gulf of Mexico Research Initiative to CSOMIO. Data are publicly available through the Gulf of Mexico Research Initiative Information and Data Cooperative (GRIIDC) at <https://data.gulfresearchinitiative.org>.

Corresponding Author:

Leiping Ye
Center for Applied Coastal Research,
University of Delaware
259 Academy Street, Room 205
Newark, DE 19716
Email: lye@udel.edu

References

- Baugh, J.V., & Manning, A.J. 2007. An assessment of a new settling velocity parameterisation for cohesive sediment transport modelling. *Cont Shelf Res.* 27:1835-55. <https://doi.org/10.1016/j.csr.2007.03.003>.
- Benson, T., & Manning, A.J. 2013. DigiFloc: The development of semi-automatic software to determine the size and settling velocity of flocs (HR Wallingford Report DDY0427-RT001).
- Daly, K.L., Passow, U., Chanton, J., & Hollander, D. 2016. Assessing the impacts of oil-associated marine snow formation and sedimentation during and after the Deepwater Horizon oil spill. *Anthropocene.* 13(2016):18-33. <https://doi.org/10.1016/j.ancene.2016.01.006>.
- Dyer, K.R., & Manning, A.J. 1999. Observation of the size, settling velocity and effective density of flocs, and their fractal dimensions.

- 297 J Sea Res. 41(1-2):87-95. [https://doi.org/](https://doi.org/10.1016/S1385-1101(98)00036-7)
298 10.1016/S1385-1101(98)00036-7.
- Q3 299 **Manning, A.J.** 2006. LabSFLOC—A labora-
300 tory system to determine the spectral charac-
301 teristics of flocculating cohesive sediments
302 (HR Wallingford Technical Report, TR 156).
- Q4 303 **Manning, A.J.** 2015. LabSFLOC-2—The
304 second generation of the laboratory system
305 to determine spectral characteristics of floccu-
306 lating cohesive and mixed sediments
307 (HR Wallingford Report).
- 308 **Manning, A.J., & Dyer, K.R.** 1999. A labo-
309 ratory examination of floc characteristics
310 with regard to turbulent shearing. *Mar Geol.*
311 160(1-2):147-70. [https://doi.org/10.1016/](https://doi.org/10.1016/S0025-3227(99)00013-4)
312 S0025-3227(99)00013-4.
- 313 **Manning, A.J., & Dyer, K.R.** 2002. The
314 use of optics for the in-situ determination of
315 flocculated mud characteristics. *J Opt Pure*
316 *Appl Opt.* 4(4):S71-81. [https://doi.org/](https://doi.org/10.1088/1464-4258/4/4/366)
317 10.1088/1464-4258/4/4/366.
- 318 **Manning, A.J., & Dyer, K.R.** 2007. Mass
319 settling flux of fine sediments in Northern
320 European estuaries: Measurements and pre-
321 dictions. *Mar Geol.* 245:107-22. [https://](https://doi.org/10.1016/j.margeo.2007.07.005)
322 doi.org/10.1016/j.margeo.2007.07.005.
- 323 **Manning, A.J., Schoellhamer, D.H., Mehta,**
324 **A.J., Nover, D., & Schladow, S.G.** 2010.
325 Video measurements of flocculated sediment
326 in lakes and estuaries in the USA. In: Pro-
327 ceedings of the 2nd Joint Federal Interagency
328 Sedimentation Conference and 4th Federal
329 Interagency Hydrologic Modeling Conference.
330 Las Vegas, NV: Joint Federal Interagency
331 Conference.
- 332 **Manning, A.J., Spearman, J.R., Whitehouse,**
333 **R.J.S., Pidduck, E.L., Baugh, J.V., & Spencer,**
334 **K.L.** 2013. Laboratory assessments of the
335 flocculation dynamics of mixed mud-sand sus-
336 pensions. In: *Sediment Transport Processes and*
337 *Their Modelling Applications*, ed. Manning,
338 A.J., 119-64. Rijeka, Croatia: InTech.
- 339 **Manning, A.J., Whitehouse, R.J.S., & Uncles,**
340 **R.J.** 2017. Suspended particulate matter: The
341 measurements of flocs. In: *ECSA Practical*
342 *Handbooks on Survey and Analysis Methods:*
343 *Estuarine and Coastal Hydrography and*
344 *Sedimentology*, eds. Uncles, R.J., & Mitchell, S.,
345 211-60. Cambridge, UK: Cambridge
346 University Press. [https://doi.org/10.1017/](https://doi.org/10.1017/9781139644426)
347 9781139644426.
- 348 **Muschenheim, D.K., & Lee, K.** 2002.
349 Removal of oil from the sea surface through
350 particulate interactions: review and prospec-
351 tus. *Spill Sci Technol B.* 8(1):9-18. [https://](https://doi.org/10.1016/S1353-2561(02)00129-9)
352 doi.org/10.1016/S1353-2561(02)00129-9.
- 353 **Passow, U., & Ziervogel, K.** 2016. Marine
354 snow sedimented oil released during the
355 Deepwater Horizon spill. *Oceanography.*
356 29(3):118-25. [https://doi.org/10.5670/oceanog.](https://doi.org/10.5670/oceanog.2016.76)
357 2016.76.
- 358 **Soulsby, R.L., Manning, A.J., Spearman, J.,**
359 **& Whitehouse, R.J.S.** 2013. Settling velocity
360 and mass settling flux of flocculated estuarine
361 sediments. *Mar Geol.* 339:1-12. [https://](https://doi.org/10.1016/j.margeo.2013.04.006)
362 doi.org/10.1016/j.margeo.2013.04.006.
- 363 **Stokes, G.G.** 1851. On the effect of the
364 internal friction on the motion of pendulums.
365 *Trans Camb Phil Soc.* 9:8-106.